APPLICATIONS OF CYCLOTRONS IN NUCLEAR PHYSICS

C. Mayer-Böricke

Institute for Nuclear Physics of Kernforschungsanlage Jülich, 517 Jülich, W. Germany

Abstract

Recent investigations on reaction mechanisms and on highly excited states in nuclei are reviewed, mainly in the fields of scattering, precompound- and compound processes, high-spin-states and giant resonances. It is shown that the high and variable energies of modern cyclotrons and the possible high energy resolution and precision was essential for the success of these experiments.

Introduction

In recent years AVF cyclotrons have proved to be very powerful tools for nuclear research due to their features of energy variability, energy precision and resolution as well as due to the growing availability of higher energies for different kinds of projectiles. In this short talk I can give, of course, only some examples of the progress in nuclear physics achieved by the use of cyclotrons and I apologize in advance that many other interesting results can not be mentioned.

In the first section I want to review some experiments with respect to

Resolution in Particle Spectra.

Nowadays, nuclear reaction and scattering experiments with cyclotrons are mostly performed using solid state detectors for the identification and energy determination of reaction products and of scattered particles.

The best energy resolution obtained with solid state detectors for high energy particles in the 100 MeV region is about $\Delta E/E = 3\cdot 10^{-4}$ (FWHM). This is illustrated in fig. 1 for the case of elastic α-scattering from Au at an incident energy of 155 MeV and a scattering angle of $\Theta_{Lab}=15^{\circ}$ [1].

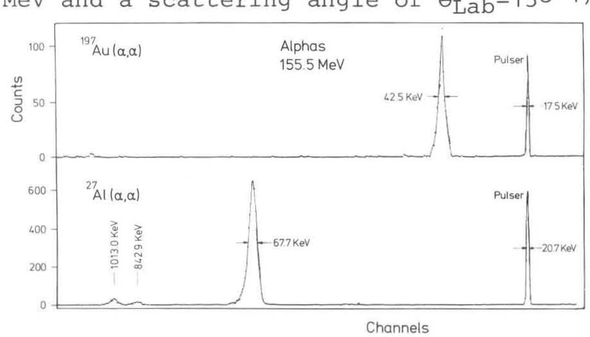

Figure 1: Spectra of scattered α-particles obtained with a Ge-detector[1].

The measured half-width of the elastic line in the upper spectrum corresponds to an energy resolution of $\Delta E/E=2.7\cdot 10^{-4}$. The detector was made of high purity germanium of 10 mm depletion depth. The lower part of fig. 1 shows an α-scattering spectrum of ^{27}Al. The kinematical contributions to the half width were strongly reduced in this case by appropriate beam matching. The FWHM of 67.7 keV corresponds to an energy resolution of $\Delta E/E=4.4\cdot 10^{-4}$.

For long range higher energy reaction particles, e.g. protons of 80 MeV, the only suitable detector type is that of side entry geometry. With a Ge(Li)-detector of appr. 30 mm length and an entrance window of $10\cdot 10$ mm^2, an energy resolution $\Delta E/E=4.1\cdot 10^{-4}$ was achieved in case of a (d,p) reaction on ^{62}Ni at 84 MeV incident energy[2].

Since cyclotron beams have usually a phase volume which is much larger than that of Tandem Van de Graaff beams, the kinematic broadening of lines in the particle spectra is quite strong for reactions and scattering processes involving light targets. If solid state detectors are used, this broadening can be easily 10 times larger than the intrinsic resolution of the detector. This problem can be tackled by appropriate beam matching. For this matching, the beam focus is no longer on the target but is shifted away from the target by appr. the distance between target and detector. The improvement achieved in resolution is demonstrated in fig. 2. The upper right hand part shows the "unmatched" spectrum of elastic α-scattering lines from

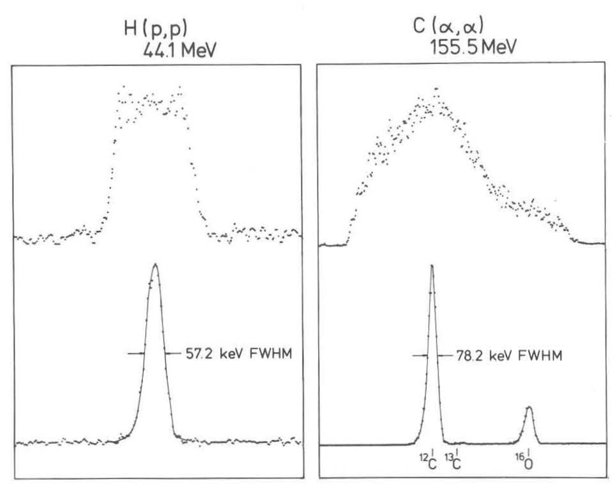

Figure 2: Improvement of energy resolution by proper beam matching[3].

Proc. 7th Int. Conf. on Cyclotrons and their Applications (Birkhäuser, Basel, 1975), p. 481-487

^{12}C and ^{16}O at 155 MeV; the lower part obtained with matching, shows a measured FWHM of 78.2 keV corresponding to an energy resolution of $\Delta E/E = 5 \cdot 10^{-4}$. Similarly, on the left hand, the matching effect for H(p,p) scattering at 44 MeV is shown[3].

Beside solid-state detectors, magnet spectrographs are used for reaction and scattering investigations. Their extremely high resolution is needed in many cases for separation of closely neighbouring lines in the particle spectra. Fig. 3 shows in the

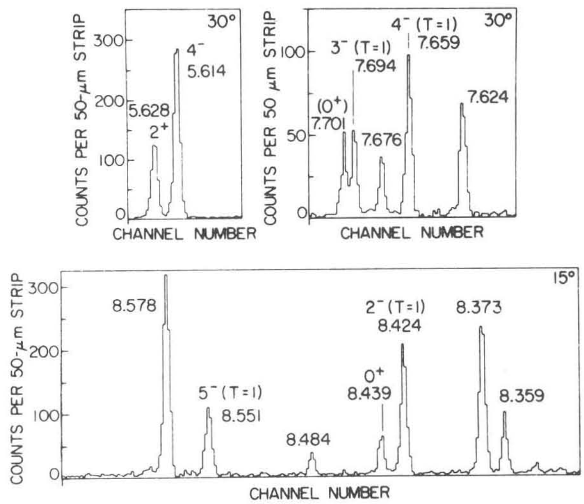

Figure 3: Closely lying inelastic scattering groups from $^{40}Ca(p,p')$ at 35 MeV incident p-energy resolved with a magnet-spectrograph[4].

upper left part, as an example, two lines in the spectrum of inelastic p-scattering from ^{40}Ca at an incident energy of 35 MeV. The line width (FWHM) of about 4.5 keV corresponds to an energy resolution of $\Delta E/E = 1.3 \cdot 10^{-4}$ [4]. The distance between these lines is only 16 keV. The 4^- state has a particle-hole structure $(f_{7/2}, d_{3/2}^{-1})$ T=0. Cross sections of about a few hundred μb for the excitation of several such previously unresolved particle-hole states have been measured in this investigation at MSU[4]. On the other hand, these measurements have been done only at the two lab angles of 15° and 30° mainly because of the time consuming scanning procedures of the plates. The precision in the energy determination of the excited levels was very high, i.e. typically between 0.3 and 1 keV for excitation energies up to about 9 MeV.

Elastic Scattering and Optical Model

For an investigation of elastic scattering in terms of the optical model complete angular distributions have to be measured. It has been shown in the last few years that in some cases the α-nucleus optical potentials can be uniquely determined at sufficiently high incident energies.

These results provide information about the gross features of the nuclei, i.e. about their radii, surface diffusenesses, potential depths, and general absorption properties of the incoming particles. Fig. 4 shows, as an example, an experimental angular distribution of 100 MeV α-scattering from ^{44}Ca together with a theoretical curve[5]

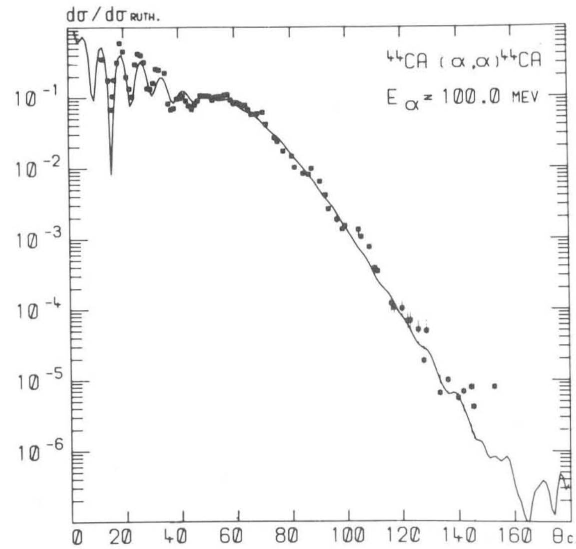

Figure 4: Angular distribution of elastic α-scattering from ^{44}Ca at 100 MeV and Optical model fit[5].

The cross-section has been measured in the angular region $16^\circ \leq \theta_{LAB} \leq 166^\circ$ where it decreases over many orders of magnitude. These data have been analyzed in terms of a 6-parameter optical model. It was found that some potentials, in spite of being able to fit the measured curve up to 70° equally well, fail to fit the data at backward angles often by orders of magnitude. Consequently no discrete potential ambiguities remained at this high incident energy, i.e. only one single parameter family turned out to be superior to all others (V=126 MeV; r_R=1.2 fm; a_R=0.8 fm; W=24.5 MeV; r_I=1.55 fm; a_I=0.64 fm).

In the next section I shall discuss

Precompound- and Compound Nuclear Reactions

With the advance of higher and variable energy beams, new reactions could be studied in which many nucleons are emitted e.g. reactions of the type (α,xn) or (α,pxn) with x running up to more than 10.

It has been known for a long time that for small x, compound-reaction processes, which involve heating up of the total intermediate nuclear system and finally boiling off of particles are an important feature of such nuclear reactions at low incident energies. Usually the continuous part of the particle spectrum was explained on this basis. However, in the last few years it turned out that the excitation functions of e.g. (α,xn) reactions, showed a completely different and unexpected behaviour at higher energies than predicted by compound reaction mechanisms. This can be seen in fig. 5. The upper part shows the experimental excitation functions of (α,xn) reactions for a ^{197}Au target over an energy range from 65 to 170 MeV[6]. All these curves show a sharp rise at lower energies, and are furthermore characterized by a broad maximum and a long flat tail extending to high energies.

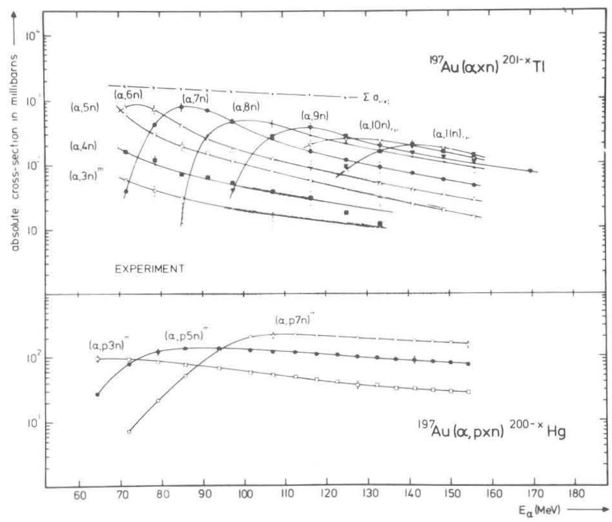

Figure 5: Experimental excitation functions of (α,xn)- and (α,pxn)-reactions in the energy range from 65 to 170 MeV[6].

The first part of these curves in the region of the maximum can be explained by the usual compound nuclear theory; however, the high energy tail was found to be a completely new feature of these reactions which could not be understood in the framework of this theory.

An explanation is given in terms of precompound processes producing high energy particles. These processes take place in the very early steps of the interaction between the incoming particle and the target nucleus. Let us assume that it takes several successive interactions or collisions until finally the energy in the total system is well distributed over many nucleons so that we can speak of a thermal equilibrium system, i.e. a compound nucleus.

How do these initial steps look like? Generally, the first interaction of the α-particle with a nucleon of the target produces a particle-hole state. This simple configuration may hold very high energy. Therefore, there is a chance that a nucleon is emitted directly out of this precompound state as a high energy "precompound particle". On the other hand it may be that by a second interaction with another nucleon in the target nucleus a second particle-hole pair is created; in this way the energy gets distributed over a larger assembly of particles. Both processes happen with a certain probability and therefore we can expect in the initial steps of the interaction, on the one hand, an emission of high energy precompound particles constituting the hard component in the corresponding particle spectra and producing the high energy tail in the excitation function; on the other hand, the equilibration process goes on until thermal equilibrium is reached in the system and particle emission is possible only by evaporation. In a heavy nucleus this evaporation is limited essentially to neutron emission, since the protons have not high enough energy to tunnel through the Coulomb-barrier of the nucleus. However, for precompound states with their high energy per excited nucleon this is no problem. Therefore we expect generally in the region of the high energy tail, e.g. of an (α,8n) reaction, to find also a comparable cross section for the (α,p7n) reaction. Actually, the epxeriments show just this feature, as can be seen in the lower part of fig. 5.

Recent hybrid model theory incorporates both processes, the predominantly high energy nucleon emission from pre-equilibrium states and the particle emission from the final equilibrium states[7]. It provides a surprisingly good overall description of all these very extended (α,xn) and (α,pxn) excitation functions and, most important, without adjustment it predicts correctly the ratio of the cross sections for (α,xn) and (α,pxn) reactions.

Many new features of highly excited states, especially their level densities at high excitation energy and the structure of precompound states can be learned from such type of investigations. For instance the initial exciton configuration n_o, i.e. the initial number of excited particle and hole states, strongly influences the shape of these yield curves. It was found in this case (fig. 5) to be n_o = 5 with a 3n-2p-0h configuration.

The (α,xn) reactions are of basic importance also for the next topic I am going to discuss.

High Spin States

In recent years a new field of research was opened concerning nuclear states of high angular momentum. In 1971 Johnson and coworkers[8,9] discovered in an experiment at the Stockholm cyclotron that there exist interesting anomalies in the level spacings of rotational ground state bands. These "backbending effects" have been investigated since in many laboratories.

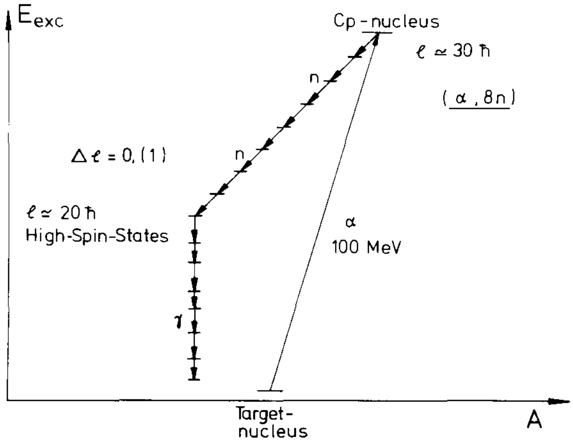

Figure 6: Scheme of an $(\alpha,8n\gamma)$-reaction exciting high spin states in the final nucleus.

For the excitation of such high spin states, reactions of the type (α,xn) at high incident energy have mostly been used, because in this way a large amount of angular momentum can be transferred to the compound nucleus (fig. 6). After emission of some neutrons, which carry away only a small amount of the total nuclear spin, the final nucleus is left in a state of high angular momentum which decays by γ-transitions into the high spin rotational states. These rotational states deexcite again by γ-transitions within the rotational band; they can be studied therefore in on-line γ-experiments.

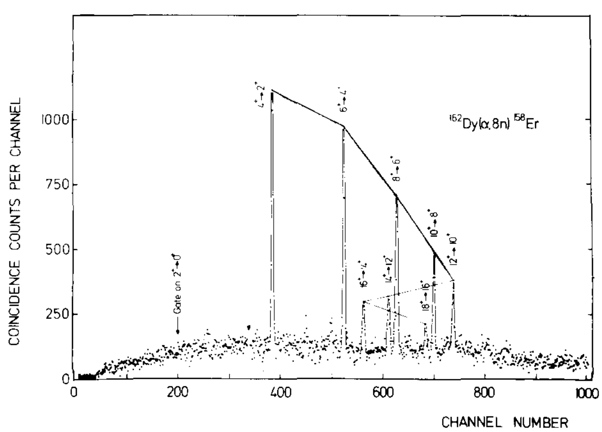

Figure 7: γ-coincidence spectrum with coincidence gate set on the 2 → 0 transition for ^{158}Er rotational transitions.

Fig. 7 shows as an example a coincidence spectrum of the ^{158}Er rotational γ-transitions gated on the 2 → 0 line[10]. This nucleus is strongly deformed and therefore the rotational transition energies shown here can be described by the simple expression

$$\Delta E_I = E_I - E_{I-2} = \frac{\hbar^2}{2\Theta}\,(4I-2).$$

I and I-2 denote the spins of the rotational levels involved in the γ-transition. Evidently, the moment of inertia Θ of the rotational nucleus can be determined experimentally for each transition from the measured transition energy ΔE_I and the spin-value I.

If Θ is assumed to be constant or only slightly increasing with I, then we expect a gradual increase of the transition energy ΔE_I with increasing I values. This feature is displayed here for the "lower" transitions 4 → 2, 6 → 4 ... up to 12 → 10. Then, however, the spectrum shows a "backbending" of the γ-energies for the 14 → 12 and 16 → 14 lines and finally again an increase of the γ-energy for the 18 → 16 transition. According to the above formula for the transition energies this means that the nuclear moment of inertia Θ increases at these high spin values suddenly and strongly and stabilizes then at this higher level.

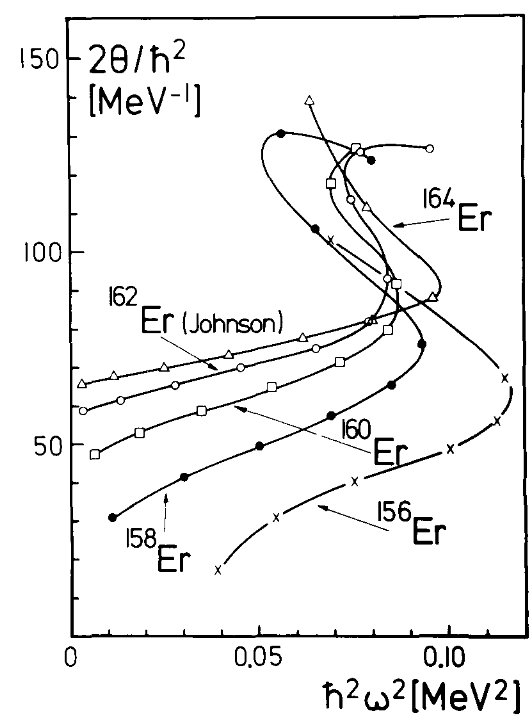

Figure 8: Θ vs. ω^2 plot of several Er-isotopes showing the "phase transition" from small to large Θ-values.

Fig. 8 shows the experimental values of the moment of inertia for different nuclei as a function of the square of the rotational frequency ω, i.e. in a "backbending plot". The measurements have been done in Stockholm, Brookhaven, Jülich and Manchester[9-14]. The first point on the left hand of the ^{158}Er plot corresponds to the Θ-value of the 2^+ rotational state, the next one to that of the 4^+ state and so on up to the last point showing the Θ-value of the 18^+ state. As can be seen from this picture all curves show a sudden increase of the moment of inertia around spin values of 10 or 12. This effect was attributed in early theoretical work[15] to a "phase transition" in nuclear matter due to the break up of nucleon pairs by the action of Coriolis forces. The idea was the following. The pairing correlations cause the small Θ-value for the ground state which is only about 50 % of the rigid rotor moment of inertia Θ_{rig}. As soon as the correlations collapse by the effect of Coriolis forces on the nucleon pairs, a sudden transition to the rigid rotor rotational band with its large Θ value is taking place in the framework of this Coriolis Anti-Pairing model (CAP)[15].

More generally speaking, the "phase transition" can be understood in terms of the crossing of two rotational bands with largely different moment of inertia. In another theoretical approach the high-Θ band is described as a rotational band based on an $(i_{13/2})^2$ 2qp neutron pair configuration which is aligned as far as possible parallel to the rotational axis by the effect of Coriolis forces (Rotation-alignment)[16]. As it stands now, both effects, CAP and rotation-alignment are contributing to the explanation of these curves.

Many interesting problems have been investigated meanwhile in this field of high spin states, mostly with respect to the mechanism of backbending and to the structure of these highly excited states. As an example, I just want to mention that investigations of neighbouring even and odd deformed Er- and Dy-nuclei showed that the backbending effect in these nuclei is produced only by neutrons.

Giant Resonances

The last topic I want to discuss shortly is giant resonances. By the use of cyclotron beams, new higher multipole giant resonances have been discovered, predominantly of quadrupole character. In medium weight and heavy nuclei this E2 giant resonance was found to have a few MeV lower excitation energy than that of the well known giant dipole resonance.

There are mainly two methods to study these highly excited simple structured nuclear states. The first one makes use of the possibility that such unbound states can be excited by direct inelastic scattering; they show up in the spectra of inelastic scattered particles as broad bumps at high excitation energies. Such experiments have been done recently in several cyclotron laboratories, e.g. at the University of Maryland, at Texas A&M University and ORNL, at Groningen University and

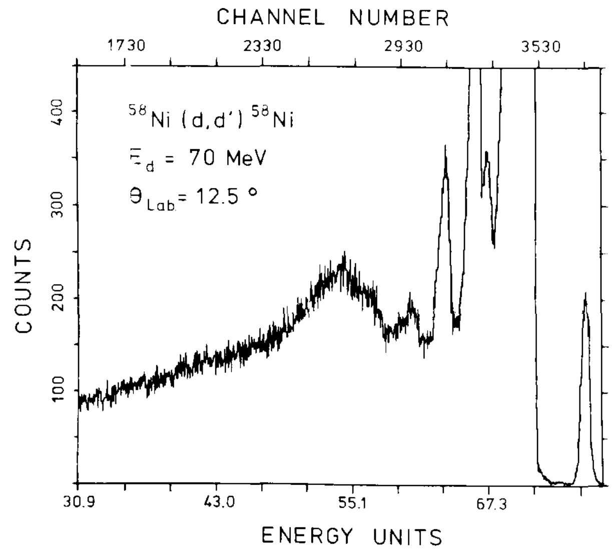

Figure 9: E2 giant resonance observed in the spectrum of inelastic d-scattering from ^{58}Ni in the energy range between 50 and 55 units with the peak at 16 MeV excitation energy[18].

at the KFA Jülich. A nice example of such a spectrum measured at Maryland University[17] is shown in fig. 9.

The broad maximum interpreted as the E2 giant resonance, is seen at an excitation energy of about 16 MeV. This corresponds to the theoretical prediction $E_x \simeq 63 \cdot A^{-1/3}$ for the excitation energy of a giant E2 isoscalar quadrupole resonance[18].

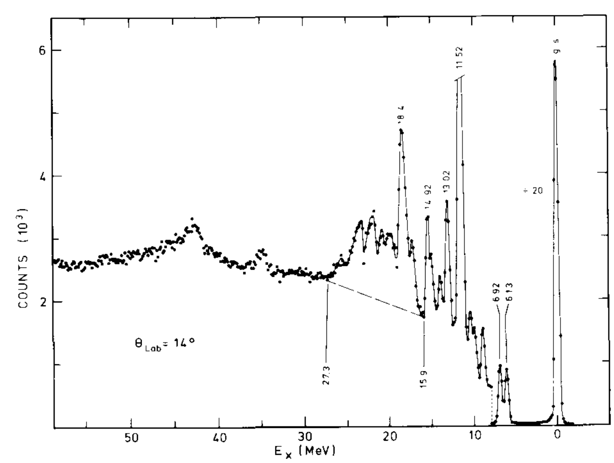

Figure 10: E2 giant resonance between 15.9 and 27.3 MeV excitation energy in ^{16}O[19].

In light nuclei, the T=O E2 quadrupole resonance shows structure and its strength is much more spread out than in medium weight nuclei; in addition its average excitation energy is shifted to smaller values than predicted by the simple formula ($63 \cdot A^{-1/3}$). Fig. 10 shows as an example a spectrum of inelastic α-scattering on ^{16}O at 146 MeV[19]. The giant resonance structure is located between 15.9 and 27.3 MeV excitation energy.

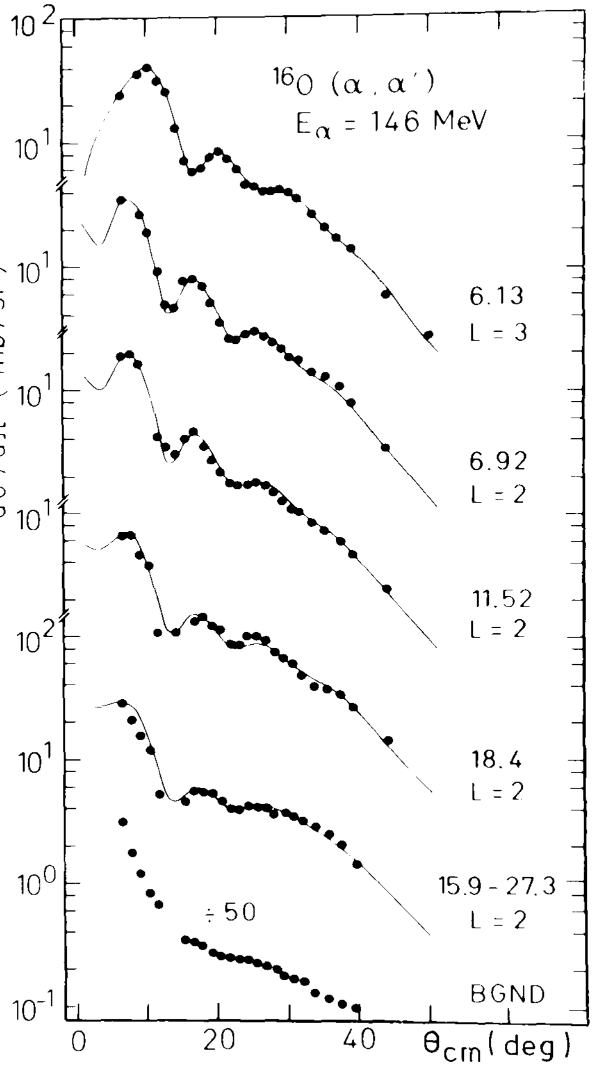

Figure 11: Measured angular distributions of inelastic α-scattering from ^{16}O exciting different states, including the distribution of the E2 giant resonance (15.9 - 27.3 MeV). The curves are DWBA-fits.

Fig. 11 shows the angular distributions of the states observed in this spectrum together with the angular distribution of the giant resonance structure between 15.9 and 27.3 MeV excitation. The curves are theoretical DWBA fits to the data. Obviously, the giant resonance angular distribution is fitted perfectly by the L=2 curve. This indicates its quadrupole nature.

The second method of investigation of giant resonances via inelastic scattering makes use of a special two step process in the scattering involving an exchange[20]. In the first step, the giant resonance is excited. In this way the incoming particle looses a large amount of energy and is therefore captured into an excited, but bound state b. In the second step the giant resonance state decays by creating a hole state d^{-1} and an outgoing particle of the same nature as the incoming one. The final nucleus is left therefore in the excited bound state bd^{-1}. Altogether an inelastic scattering to this bound state, mediated by the virtual formation of the giant resonance has taken place. The effect of the giant resonance is seen mainly in such cases, where the normal inelastic scattering amplitude for excitation of the

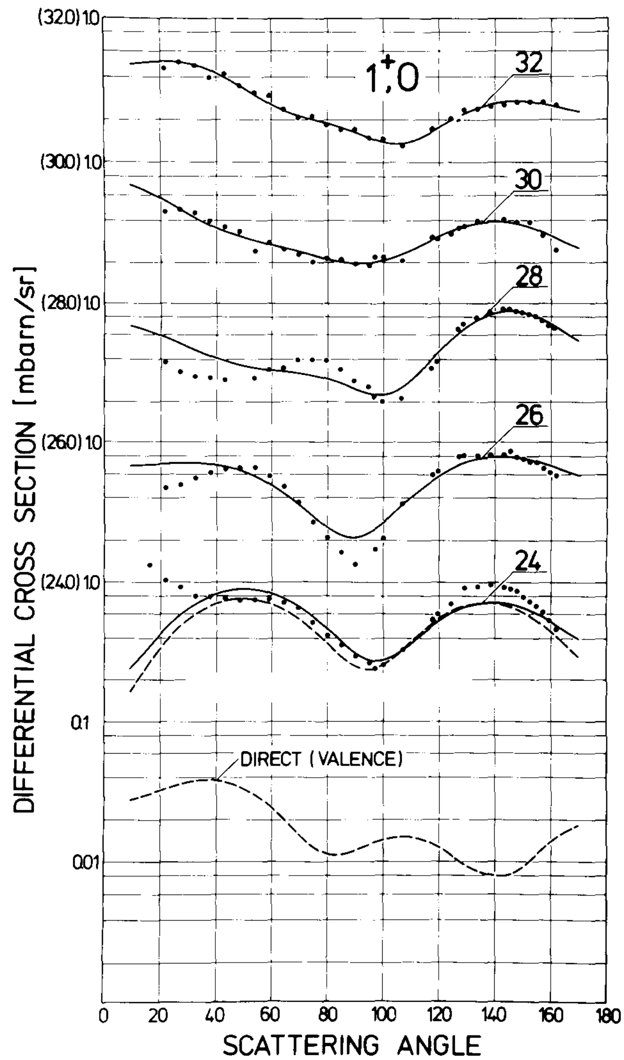

Figure 12: Angular distributions of inelastic p-scattering exciting the ^{12}C 1^+ state at 15.11 MeV together with the corresponding theoretical curves.

bound state bd^{-1} is small so that second order processes show up more clearly. This is the case for states with unnatural spin parity combination e.g. 1^+.

Experimentally, angular distributions of inelastic scattering to such a state have to be measured. If the incident energy is just appropriate for virtual excitation of the giant resonance, the shape of the angular distribution is strongly affected. Fig. 12 shows an example for inelastic proton scattering from ^{12}C to the 1^+ state at 15.11 MeV. The direct inelastic scattering is negligible. However, the measured angular distribution is fitted well by the second order calculations including the virtual excitation of the giant resonance (full lines). As compared to the calculated normal inelastic angular distribution (direct), the experimental angular distribution is of different shape and the cross section is strongly increased.

Since giant resonances are several MeV wide, angular distributions have to be measured in small steps for a set of incident energies. Fig. 12 gives only a small fraction of the measured data. This is therefore another fine example for the use of variable energy cyclotrons in nuclear physics. From the angular distributions, the strength distributions of the giant resonances (E1 and E2) can be extracted by a theoretical analysis (fig. 13).

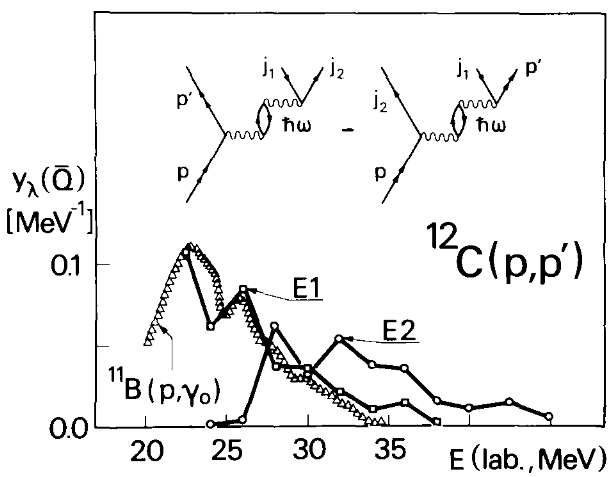

Figure 13: $Y_1(\bar{Q})$ and $Y_2(\bar{Q})$ representing the strength distributions as extracted from (p,p')-experiments[20]. The giant resonance result from $^{11}B(p,\gamma_0)$ is shown for comparison.

References

1) G. Riepe, D. Protić, J. Reich, KFA Jülich, unpublished.

2) G. Riepe and D. Protić, IEEE Trans. Nucl. Sc. Ns-22 (1975) 178.

3) J. Reich, S. Martin, D. Protić, G. Riepe, contribution to this conference.

4) J.A. Nolen, Jr. and R.J. Gleitmann, Phys. Rev. C, 11 (1975) 1159.

5) H. Eickhoff et al., Univ. of Münster and KFA Jülich, to be published.

6) A. Djaloeis et al., KFA Jülich, to be published.

7) M. Blann and A. Mignerey, Nucl. Phys. A186 (1972) 245.

8) A. Johnson, H. Ryde, and J. Sztarkier, Phys. Lett. 34B (1971) 605.

9) A. Johnson, H. Ryde, and S.A. Hjorth, Nucl. Phys. A197 (1972) 753.

10) H. Beuscher et al., Phys. Lett. 40B (1972) 449.

11) H. Beuscher et al., Z. Phys. 263 (1973) 201.

12) H. Ryde et al., Nucl. Phys. A207 (1973) 513.

13) A.W. Sunyar et al., Contrib. to the Symp. on High Spin Nuclear States and Related Phenomena, Stockholm, 1972.

14) J.C. Lisle et al., Proc. of Int. Conf. on Nucl. Phys., Munich, 1973, ed. by J. de Boer and H.J. Mang (North Holland) p. 187.

15) B.R. Mottelson and J.G. Valatin, Phys. Rev. Lett. 5 (1960) 511.

16) F.S. Stephens and R.S. Simon, Nucl. Phys. A183 (1972) 257.

17) G.F. Burdzik et al., (Maryland Univ.) and F.E. Bertrand et al. (ORNL), Univ. of Maryland, Cycl. Lab., Progress Report 1974, p. 30.

18) A. Bohr and B.R. Mottelson, Nuclear Structure (Benjamin, New York, to be published), Vol. II, Chapter 6.

19) H. Breuer et al., Proc. of the Symp. on Highly Excited States in Nuclei, KFA Jülich, September 1975.

20) H.V. v. Geramb et al., Nucl. Phys. A199 (1973) 545.